

Identification of Critical Clusters in Inverter-based Microgrids

Andrey Gorbunov

Jimmy Chih-Hsien Peng

The Department of Electrical & Computer Engineering
The National University of Singapore
Singapore
gorbunov@u.nus.edu, jpeng@nus.edu.sg

Petr Vorobev

Center for Energy Science and Technology
Skolkovo Institute of Science of Technology
Moscow, Russia
p.vorobev@skoltech.ru

Abstract—In this paper, we investigate the stability properties of inverter-based microgrids by establishing the possible presence of the so-called critical clusters - groups of inverters with their control settings being close to the stability boundary. For this, we consider the spectrum of the weighted admittance matrix of the network and show that its distinct eigenvalues correspond to inverter clusters, whose structure can be revealed by the corresponding eigenvector. We show that the maximum eigenvalue of the weighted admittance matrix corresponds to the cluster, closest to stability boundary. We also establish, that there exists a boundary on the value of this eigenvalue, that corresponds to the stability of the overall system. Thus, we make it possible to certify the stability of the system and find the groups of inverters which control settings are closest to the stability boundary.

Index Terms—inverter-based microgrids, droop controlled inverters, small signal stability.

I. INTRODUCTION

Grid-forming inverters are thought to be the core technology for inverter-based microgrids, allowing them to operate in stand-alone modes without being connected to the main power grid. For a microgrid to be secure with respect to a sudden loss of any single inverter, it is required that more than one of its inverters is continuously operating in the grid forming mode. Ideally, it is best to have all inverters (those that are dispatchable) operating in such grid-forming mode as this will maximize the reliability of the microgrid to provide uninterrupted services to consumers. On the other hand, the parallel operation of grid-forming inverters is not possible if they all attempt to keep certain constant frequency, so special control systems are needed to ensure their stable operation.

Droop-controlled inverters [1] are designed to mimic the dynamic behavior of synchronous generators by intentionally adjusting their output frequency in response to change in real power output. It can be shown, that from the point of the power system, such an inverter is fully equivalent to a synchronous machine, and dynamic equations for inverter frequency is similar to swing equation for the machine. However, experimental results [2] showed, that droop-controlled inverters, working in parallel, are prone to instabilities and the allowed region for values of droop coefficients can be quite restricted. Further analysis of such systems revealed that conventional approaches for analysing dynamics of power systems based on timescales

separation, where the slower modes associated with power controllers can be considered separately from the fast network dynamics fail to perform well for inverter-based microgrids [3]. It was shown, that the fast electro-magnetic dynamics of the network can not be neglected when analysing the small-signal stability for power controllers, thus making the dynamic model of the system very complex [4], since all the line currents have to be modeled as dynamic states.

Recently, there was an extensive research activity dedicated to model order reduction techniques suitable for microgrids. The main questions that were targeted are simplified models efficient for subsequent numerical analysis [5], identification of the degrees of freedom to exclude [4], analytic models with further instability analysis [6]. It was established that the instabilities in inverter-based microgrids have extraordinary nature and do not have an analogy in large-scale power systems. In particular, it was found that shorter network lines and more significant values of droop coefficients of the inverters tend to promote instabilities. In [4] the term "critical clusters" was used to refer to a group of adjacent inverters that are tightly connected and make the dominant contribution to the unstable mode. It is thus essential, to identify these critical clusters since it is the parameters of this group that need to be modified to restore the system's stability or enhance its stability margin. Identification of critical clusters can be challenging (even if the full-scale direct numerical stability analysis is performed) since their proximity to the instability onset depends on both the network parameters and the inverter control settings. In particular, it is not the most tightly connected cluster that is critical, but rather the one with the unfortunate combination of line parameters and droop values.

In the present manuscript, we develop a method for generalization of the critical clusters concept: we find an equivalent representation for a microgrid as a set of clusters, that are ranked according to their "criticality." Each of the clusters appears to be equivalent to an inverter-infinite bus system with some effective parameters, that makes the stability analysis straightforward. Such a representation becomes possible by analysing the system susceptance matrix, which is first multiplied by a matrix of inverter droop coefficients. We show, that every eigenvalue of such a "weighted" susceptance

matrix correspond to one cluster, and clusters can be naturally arranged in the order of their "criticality" according to the corresponding eigenvalues. After the clusters are identified, we can immediately determine whether the system is stable and specify the parameters that need to be changed to stabilize the system or enhance its stability.

The paper proceeds as follows. Section II introduces the dynamic model for inverter-based microgrid and derives its representation in the state-space form. Section III presents the core result of the paper - connection between the spectrum of the system weighted graph Laplacian matrix and small-signal stability, and explains how critical clusters can be identified using this spectrum. We demonstrate the stability assessment and stability enhancement method for a test system in Section IV. Concluding remarks are given in Section V.

II. DYNAMICS OF DROOP-CONTROLLED INVERTERS

Let us consider a microgrid composed of a number of droop-controlled inverters, connected with lines. Such a grid can be thought of as a graph with the set of edges \mathcal{E} corresponding to lines, and the set of nodes - \mathcal{V} , corresponding to inverters. We assume that the system is operating in a certain steady-state with an ac frequency ω_0 . For the small-signal stability studies it is then convenient to switch to the so-called dynamic phasor domain, where each AC bus voltage $v_i(t)$ and line current $i^{ik}(t)$ are represented in the following way [6], [7]:

$$v_i(t) = \text{Re}[U_i(t)e^{j\omega_0 t}]; \quad i^{ik}(t) = \text{Re}[I^{ik}(t)e^{j\omega_0 t}] \quad (1)$$

Both $U_i(t)$ and $I^{ik}(t)$ are the mentioned dynamic phasors, which can be arbitrary functions of time, not necessarily slowly varying. It is further convenient to represent them as phasors with d and q components:

$$U_i(t) = U_{d,i} + jU_{q,i} = V_i(t)e^{j\theta_i(t)} \quad (2a)$$

$$I^{ik}(t) = I_d^{ik} + jI_q^{ik} \quad (2b)$$

Using this representation, dynamics of inverter-based microgrid [8], [3] for small-signal stability studies can be described by the following set of linearized equations (for detailed discussion of the linearization procedure see [6]):

$$\dot{\theta}_i = \omega_i \quad (3a)$$

$$\tau\dot{\omega}_i = -\omega_i - m_i P_i \quad (3b)$$

$$\tau\dot{V}_i = -V_i - n_i Q_i \quad (3c)$$

$$L^{ij} \dot{I}_d^{ij} = V^i - V^j - R^{ij} I_d^{ij} + \omega_0 L^{ij} I_q^{ij} \quad (3d)$$

$$L^{ij} \dot{I}_q^{ij} = \theta^i - \theta^j - R^{ij} I_q^{ij} - \omega_0 L^{ij} I_d^{ij}, \quad (3e)$$

where all the variables with the subscript i refer to inverter at bus i ($i \in \mathcal{V}$) and all the variables with the superscripts ik refer to line between buses i and k ($(ij) \in \mathcal{E}$). Thus, V_i , θ_i , and ω_i are the (small-signal variations) of inverter i voltage, phase, and frequency respectively, P_i and Q_i are the instantaneous real and reactive power discharged by the inverter (again, small-signal variations), and m_i , n_i are frequency and voltage droop coefficients. $I_{d^{ik}}$ and $I_{q^{ik}}$ are d - and q - components of the current in line ik , and L^{ik} and R^{ik} are its inductance

and resistance respectively. Parameter τ is the inverse of the power controller low-pass filter cut-off frequency ($\tau = 1/\omega_c$), for simplicity we assume it to be the same for every inverter.

We emphasize, that according to numerous studies [8], [3], [4], [6], the fast electromagnetic dynamics, represented by equations (3d) and (3e) *can not be neglected* even when studying the stability of much slower power controller modes. Therefore, the total number of equations, that comprise the system dynamic model is $3\mathcal{M} + 2l$, where \mathcal{M} - is the total number of inverters and l is the total number of lines. In addition to equations (3), Kirchhoff's current law should be written for every virtual node in the system.

In order to perform the small-signal stability of the system (3) we first introduce its dynamic admittance matrix in the Laplace domain:

$$\hat{Y}_{ij}(s) = \begin{cases} \sum_{k \in \mathcal{V}, k \neq i} y^{ik}(s), & i = j \\ -y^{ij}(s), & i \neq j \end{cases} \quad (4)$$

Next, we assume, that all the lines in the microgrid are of the same type, i.e. have the same R/X ratio: $\frac{R^{ij}}{X^{ij}} = \rho$ for every ij . Then, the dynamic admittance matrix is proportional to the static susceptance matrix $\hat{B} = -\text{Im}(\hat{Y}(0))$, that is:

$$\hat{Y}(s) = \frac{\rho^2 + 1}{\rho + j + \frac{s}{\omega_0}} \hat{B}. \quad (5)$$

Therefore, the Kron reduction of the dynamic admittance matrix is given by $Y(s) = \frac{\rho^2 + 1}{\rho + j + \frac{s}{\omega_0}} B$, where B is the Kron reduced susceptance matrix. The transient admittance matrix $Y(s)$ is used to connect inverter bus voltages to inverter current injections in the linear approximation as:

$$(\mathbf{I}_d + j\mathbf{I}_q) = Y(s)(\mathbf{V} + j\boldsymbol{\theta}) \quad (6)$$

where \mathbf{V} , $\boldsymbol{\theta}$, \mathbf{I}_d , and \mathbf{I}_q are the \mathcal{M} -dimensional vectors of inverter voltages, phases, d - and q - output currents respectively. We also use the vector of inverter frequencies $\boldsymbol{\omega}$.

Under the assumption of small voltage and phase difference between inverters (see [6], [3]), the following relation can be written between inverter output active and reactive powers and the current components:

$$\begin{pmatrix} \mathbf{P} \\ \mathbf{Q} \end{pmatrix} = \begin{bmatrix} I & 0 \\ 0 & -I \end{bmatrix} \begin{pmatrix} \mathbf{I}_d \\ \mathbf{I}_q \end{pmatrix} \quad (7)$$

where I is the $\mathcal{M} \times \mathcal{M}$ identity matrix.

Finally, we obtain that following state-space representation for dynamics of the microgrid:

$$\dot{\mathbf{x}} = \mathbf{A}\mathbf{x} \quad (8)$$

where the state vector $\mathbf{x} = [\boldsymbol{\theta}, \boldsymbol{\omega}, \mathbf{V}, \mathbf{I}_d, \mathbf{I}_q]^T$ is a $5m$ -dimensional state vector of the system, and the state matrix \mathbf{A} is given by the following expression:

$$\mathbf{A} = \begin{bmatrix} 0 & I & 0 & 0 & 0 \\ 0 & -\omega_c I & 0 & -\omega_c M & 0 \\ 0 & 0 & -\omega_c I & 0 & \omega_c N \\ 0 & 0 & \omega_0 B' & -\omega_0 \rho I & \omega_0 I \\ \omega_0 B' & 0 & 0 & -\omega_0 I & -\omega_0 \rho I \end{bmatrix} \quad (9)$$

and we made a short-cut denotation $B' = (1 + \rho^2)B$.

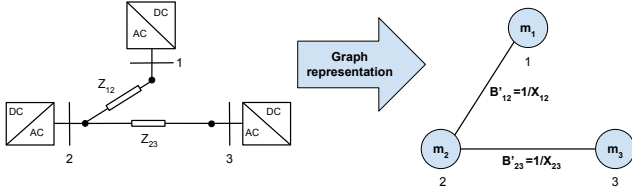


Fig. 1. Graph representation of the inverter-based microgrid

III. EIGENMODES DECOMPOSITION THEORY

In this section, we relate the spectrum of a network graph with the spectrum of the linearized model (8). Let us introduce the following weighted Laplacian matrix C of the network graph, which we will define as follows:

$$C = MB', \quad (10)$$

where susceptance matrix, $B' = -(1+\rho^2) \text{Im}(Y)$ was defined in the end of the previous section, and $M = \text{diag}(m_1, \dots, m_l)$ is the diagonal matrix of the inverter frequency droop gains. We also denote the eigenvalues of the C matrix as μ_i and the corresponding eigenvectors as \mathbf{u}_i :

$$C\mathbf{u}_i = \mu_i\mathbf{u}_i, \quad i = 1, \dots, l. \quad (11)$$

Matrix C could be considered as a 'generalized' Laplacian matrix for the network graph augmented by node weights equal to droop gains m_i , $i = 1, \dots, l$ as depicted in Fig. 1. Technically, C is not a Laplacian matrix but preserves some basic properties which are discussed below.

As an example, matrix C for the system depicted in Fig. 1 has the following explicit form:

$$C = \begin{bmatrix} \frac{m_1}{X_{12}} & -\frac{m_1}{X_{12}} & 0 \\ -\frac{m_2}{X_{12}} & m_2\left(\frac{1}{X_{12}} + \frac{1}{X_{23}}\right) & -\frac{m_2}{X_{23}} \\ 0 & -\frac{m_3}{X_{23}} & \frac{m_3}{X_{23}} \end{bmatrix}. \quad (12)$$

This example illustrates the relationship between C and the network admittance matrix Y . Precisely, C is the admittance matrix for the equivalent lossless network (setting $R = 0$) multiplied by M . One could notice from (12) that, unlike the admittance matrix, C is in general not symmetric, and the sum of the elements in each column is generally not zero. Therefore, C loses some of the properties of the admittance (weighted Laplacian) matrix.

However, it is possible to make C symmetric by a proper similarity transformation:

$$M^{-1/2}CM^{1/2} = \begin{bmatrix} \frac{m_1}{X_{12}} & -\frac{\sqrt{m_1 m_2}}{X_{12}} & 0 \\ -\frac{\sqrt{m_1 m_2}}{X_{12}} & m_2\left(\frac{1}{X_{12}} + \frac{1}{X_{23}}\right) & -\frac{\sqrt{m_2 m_3}}{X_{23}} \\ 0 & -\frac{\sqrt{m_2 m_3}}{X_{23}} & \frac{m_3}{X_{23}} \end{bmatrix}, \quad (13)$$

However, in this case, the sum of neither columns nor rows is zero, i.e., diagonal elements are not the sum of non-diagonal elements in each row and column. Although, C is not exactly a Laplacian matrix, some properties could

be inferred. For instance, $M^{-1/2}CM^{1/2}$ is positive semi-definite ($\mathbf{x}^T M^{1/2} B' M^{1/2} \mathbf{x} = (M^{1/2} \mathbf{x})^T B' (M^{1/2} \mathbf{x}) \geq 0$). Consequently, μ_i are real non-negative¹, and eigenvectors \mathbf{u}' of $M^{-1/2}CM^{1/2}$ could be chosen to be real. If \mathbf{u}' are real, then \mathbf{u} will be also real according to the similarity transformation $\mathbf{u}' = M^{-1/2}\mathbf{u}$.

The following theorem, which is one of the main contributions of the present paper, establishes the connection between the spectrum of C and the spectrum of dynamic system (8).

Theorem III.1. *If $\rho = \frac{R}{X}$ ratios are the same across the system and droop gains are proportional, $M = kN$, $k > 0$, the eigenvalues λ of the linearized system (3) (given in (8)) are connected with the eigenvalues μ of C as the follows,*

$$k g^2(\lambda)(h^2(\lambda) + 1)\lambda + g(\lambda)(k + \lambda)\mu + \mu^2 = 0 \quad (14)$$

where $g(\lambda) = (1 + \tau\lambda)$, $h(\lambda) = (\rho + \frac{1}{\omega_0})\lambda$.

Besides, the eigenvector \mathbf{u} of C coincides with the (8) eigenvector part corresponding to $\boldsymbol{\theta}$.

Proof. If R/X ratio is the same across the system and frequency and voltage droop gains ratio is the same for every inverter, i.e., $M = kN$, then the linearized system (8) is equivalent to the following matrix polynomial in the Laplace domain:

$$[k g^2(s)(h^2(s) + 1)sI + g(s)(k + s)MB' + (MB')^2]\boldsymbol{\theta} = 0 \quad (15)$$

One could verify that by expressing (8) in terms of $\boldsymbol{\theta}$ vector. Further, one could verify that \mathbf{u} is, indeed, the eigenvector for (15). \square

Remark. *Each μ corresponds to five eigenvalues λ that are the roots of (14). For example, all λ of the two-bus system depicted in Fig. 2 are the roots of (14) with one particular $\mu = \frac{m}{X}$. Hereby, the system (8) of l inverters decouples into l separate clusters each corresponding to one μ_i , $i = 1, \dots, l$.*

The fact that \mathbf{u} are real means phase shifts between any two elements of a mode shape of (8) associated with $\boldsymbol{\theta}$ (that is also \mathbf{u} according Theorem III.1) are either 0° or 180° . Therefore, one group of inverters oscillates in phase while another in the opposing phase. These two groups are called *coherent* groups in conventional power systems study [10].

Here, we demonstrate that there exists a certain threshold value of μ_{cr} , that can be used to assess the stability of the system. In fact, if any of the μ_i for a given system is greater than μ_{cr} , then the system is unstable, and vice versa. Therefore, we can use the value of the highest μ_i for the system to assess its stability. The characteristic equation (14) depends on a positive μ that could be treated as a parameter for the root locus. The root locus for dominant eigenvalue λ associated with droop control dynamics is depicted in Fig. 3 with typical parameters: $k = 1$, $\rho = 1.4$, and μ varying in the range 60-1000. The root locus shows that $\text{Re}(\lambda)$ monotonically depends

¹For the connected graph (without isolated nodes) there is only one trivial $\mu_1 = 0$ with $\mathbf{u}_1 = [1, \dots, 1]^T$. It follows from the uniqueness of trivial eigenvalue for the Laplacian B' [9] and the min-max theorem for symmetric C : $m_{\min}\lambda_i(B') \leq \mu_i \leq m_{\max}\lambda_i(B')$.

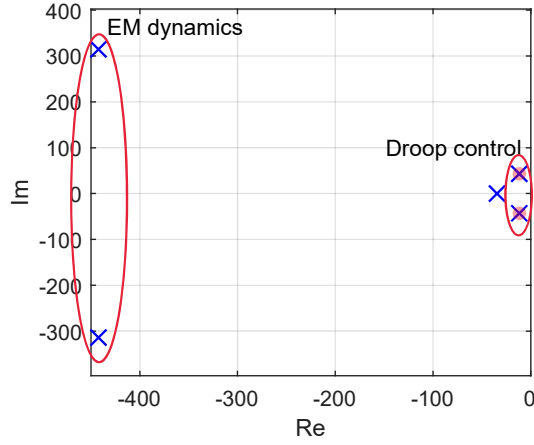


Fig. 2. An eigenplot for the two-bus system

on μ . Therefore, for each set k, ρ , there is a unique upper bound μ_{cr} that we calculate in the following section. Further, it could be inferred that the roots of (14) are stable if and only if the highest $\mu_l = \max_{\mathbf{x} \neq 0} \frac{\mathbf{x}^\dagger C \mathbf{x}}{\mathbf{x}^\dagger \mathbf{x}} < \mu_{cr}$. Therefore, μ is a parameterization of the network topology augmented with droop gains M . In other words, μ concentrates the information on corresponding cluster connectedness.

In addition, the following important Theorem holds:

Theorem III.2. *The addition of any new line or the increase of $B'_e = \frac{1}{X_e}$ (susceptance) for any existing line in the system increases eigenvalues $\mu_i, i = 1, \dots, l$.*

Proof. To check this fact for the line addition, let us consider line connection $e = (1, 2)$ without loss of generality. The new $\hat{C} = C + C_e$ is decomposed into sum of the original C for the graph without added line and C_e is the 'generalized' Laplacian of the graph on l vertices consisting of just the edge $e = (1, 2)$ with X_{12} ,

$$C_e = \frac{1}{X_{12}} \begin{pmatrix} m_1 & -m_1 & 0 & \cdots & 0 \\ -m_2 & m_2 & 0 & \cdots & 0 \\ 0 & 0 & 0 & \cdots & 0 \\ \vdots & \vdots & \vdots & \ddots & \vdots \\ 0 & 0 & 0 & \cdots & 0 \end{pmatrix}. \quad (16)$$

Then one could use Weyl's inequality for eigenvalues of the sum \hat{C} of matrices C and C_e [11]:

$$\mu_i \leq \hat{\mu}_i \leq \mu_i + \frac{m_1 + m_2}{X_{12}}, i = 1, \dots, l, \quad (17)$$

where $\hat{\mu}_i$ are eigenvalues for \hat{C} . The given argument could be applied to any line $e = (i, j)$ addition. Also, the change of the existing line $e = (i, j)$ susceptance by ΔX_e gives analogous to (16) C_e . Hence, the argument extends to the change of the existing line parameters. \square

The result of the Theorem III.2 suggests that adding a new line to the microgrid, as well as reducing the impedance values of existing lines, can only reduce the stability margin. This

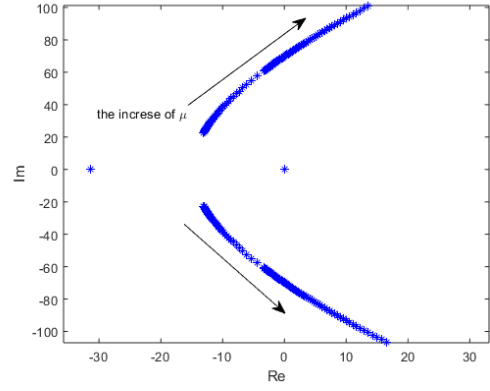


Fig. 3. Root locus for the two-bus system

result is entirely consistent with the previous findings of [6] and [7] and is specific for microgrids having no analogy in large-scale power systems.

A. Procedure for identifying critical clusters

Let us now explain how we can use the spectrum of the 'generalized' Laplacian matrix C to assess the stability of a microgrid. (We start from noticing, that both equations (14) and (15) only depend on the system R/X ratio ρ and droop gains ratio k and do not depend on the system topology and line lengths.) Therefore, the value of μ_{cr} , which can be calculated from any of these equations, also is independent of the system topology and line lengths.

Therefore, the procedure of the stability assessment is the following. We first determine μ_{cr} from (14) provided the values of ρ and k are given for our system. Next, we find the actual values of μ_i - the spectrum of the matrix C . If none of the μ_i is greater than μ_{cr} , then the system is stable. If one or more of μ_i is greater than μ_{cr} , then the system is unstable, and the corresponding eigenvectors \mathbf{u}_i gives the structure for the corresponding critical clusters. The high magnitudes of \mathbf{u}_i correspond to critical droop or line parameters. The whole procedure is described in more detail by the flow-chart in Fig. 4. The results of the above-described procedure are the list of two-bus equivalent systems, arranged in the order of decreasing μ . Those, corresponding to higher μ 's will have the most influence on the system stability, and it is the parameters of the inverters and lines in these clusters that should be changed to stabilize the system or increase its stability margin. Figure 5 illustrates the two-bus equivalent clusters on the example of a 4-bus Kundur system.

Figure 6 gives a plot for μ_{cr} as a function of ρ and k . One can notice, that the minimum boundary for $\mu_{cr} \geq 200$ provides a good estimation for a wide class of grids (unless the value of ρ is exceptionally low). We also note, there is a significant stability margin increase for the values k in the range 10 to 50 in terms of μ . This region of k is not very important for practical applications, but the results is fully consistent with the previous findings from [6].

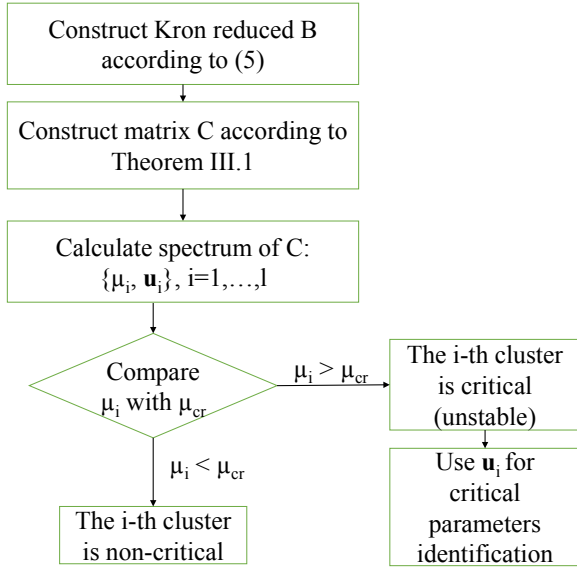


Fig. 4. Critical cluster identification

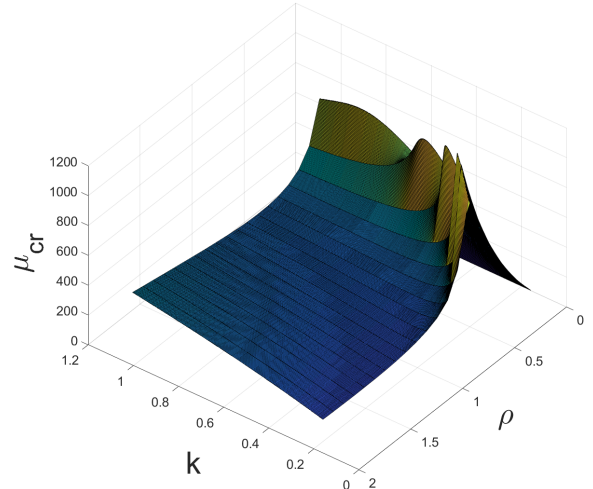


Fig. 6. Critical value of μ for range of ρ and k values.

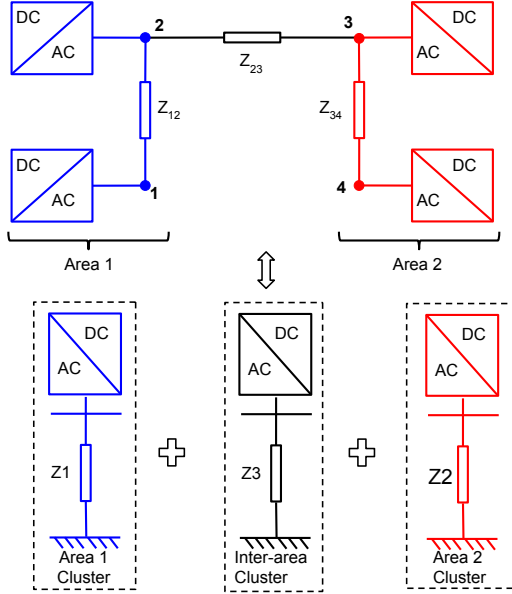


Fig. 5. The two-bus representation

IV. NUMERICAL VALIDATION

This section provides numerical validation of the procedure for critical clusters identification. In addition, we also provide an illustration of the stability enhancement procedure using the identified critical clusters. For our numerical tests, we consider the 4-bus Kundur system (Fig. 5), where each bus is supposed to be equipped with a droop controlled inverter.

A. Base test case

We start from the initial system with the parameter values given in Table I. For the values of $\rho = 1.4$ and $k = 1.0$ for our system, one finds from equation (14) that $\mu_{cr} = 195$. The

eigenvalues of the system weighted admittance matrix C for the parameters of Table are the following (apart from the trivial zero eigenvalue): $\mu_1 = 9.68$, $\mu_2 = 110.19$, $\mu_3 = 215.23$. These eigenvalues correspond to the three distinct clusters, each corresponding to pairs of neighbouring inverters, as depicted in Fig.5.

We see that one of the eigenvalues - μ_3 is greater than μ_{cr} for this system. Therefore, the system is unstable. The eigenvector, corresponding to this value is $u_2 = [-0.018, 0.056, -0.725, 0.687]^T$. We deduce that the critical cluster is composed of inverters 3 and 4, which is also illustrated in Fig. 5. Therefore, it is the values of droop gains of these inverters and the impedance of the line 3 – 4 that have the most effect on the system stability, and one needs to modify them to stabilize the system.

TABLE I
PARAMETERS OF THE FOUR-INVERTER SYSTEM

Parameter	Description	Value
ω_0	Nominal Frequency	$2\pi 50 \text{ rads/s}$
U_b	Base Voltage	230 V
S_b	Base Inverter Rating	10kVA
ρ	R/X ratio	1.4
k	Droop gain ratio	1
R	Line Resistance	$222.2 \text{ m}\Omega/\text{km}$
L	Line Inductance	$0.51 \text{ mH}/\text{km}$
m_i	Frequency Droop Gain	1%
n_i	Voltage Droop Gain	1%
l_{12}	Line 1-2 length	6 km
l_{23}	Line 2-3 length	30 km
l_{34}	Line 3-4 length	3 km

B. Line parameters variations

Firstly, we illustrate the system stabilization by changing the impedance of the line between inverters 3 and 4 (according to critical cluster structure). Fig. 7 shows the dependence of all μ values on the length of the 3 – 4 line l_{34} , or, equivalently,

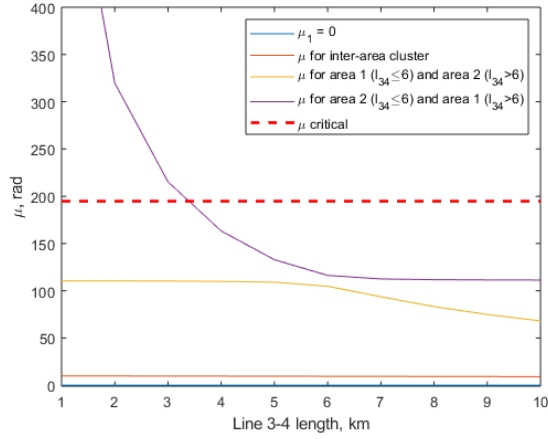


Fig. 7. Variation μ with respect to line 3-4 length, l_{34}

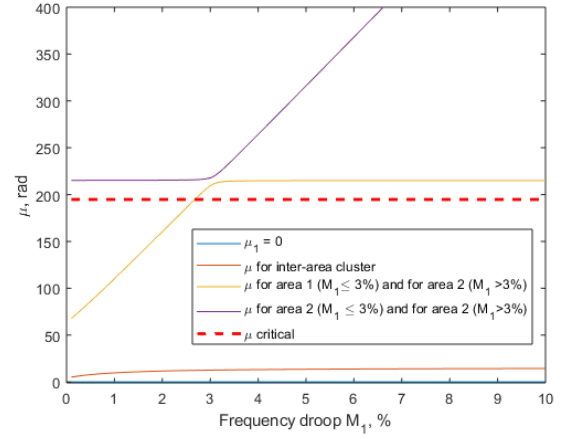


Fig. 9. Variation μ with respect to the first frequency droop gain, M_1

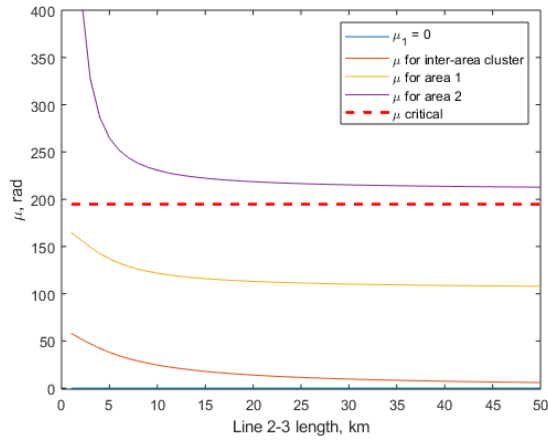


Fig. 8. Variation μ with respect to line 2-3 length, l_{23}

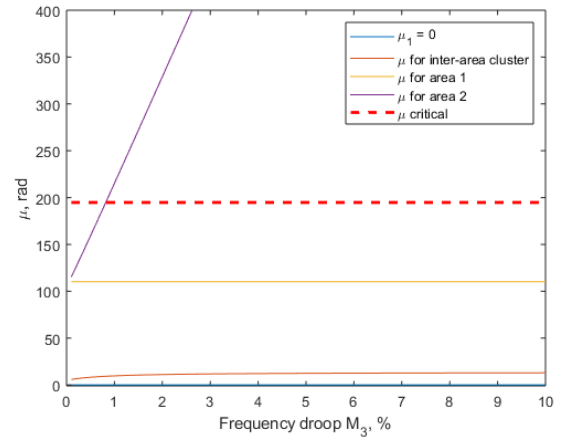


Fig. 10. Variation μ with respect to the second frequency droop gain, M_3

on its impedance value. We observe that for the values of the line length smaller than about 6 km, only the μ_2 value - the critical one is affected. The system gains stability starting from the length of this line around 3.3 km, which is slightly higher than the starting value for this line. The system remains stable for l_{34} bigger than this value.

On the other hand, Fig. 8, that the variation of the line 2 – 3 length, even in a much higher range - up to 50 km could not stabilize the system as μ_3 stays above the critical value. This is the consequence of the fact that the cluster 3 remains unstable even for an infinite length of the line 2 – 3 when the system splits into two separate areas.

C. Droop gains variations

Secondly, we show that the system can also be stabilized by changing the droop gains of inverters 3 and/or 4. Fig. 9 shows the dependence of the eigenvalues μ on the M_1 - frequency droop of inverter 1. We see that across all the region of the values of M_1 , the value of μ_3 stays above μ_{cr} . Therefore, it is impossible to stabilize the system by any variations of the droop gains of inverter 1. This is in agreement with the

fact that the cluster, responsible for instability, is composed of inverters 3 and 4. Moreover, with the increase of M_1 above a certain threshold ($\sim 3\%$), another eigenvalue, namely, μ_1 crosses the critical value, so that the system now has two critical clusters, making it unstable.

The situation is different, with the variation of the inverter 3 droop gain M_3 . Fig. 10 demonstrates, that the value of μ_2 is greatly affected by this variation, so the system can be efficiently stabilized by adjusting (decreasing) the M_3 coefficient.

V. CONCLUSIONS AND FUTURE WORK

We have developed a method for stability assessment of inverter-based microgrids by means of representing it as a set of 2-bus equivalent clusters, which can be arranged in order of their proximity to instability. The method is based on the analysis of the spectrum of a special weighted admittance matrix of the network and determining the eigenvalues, that lie above a certain threshold. Our findings are consistent with the number of previous results on account of the fact that groups of tightly connected neighboring inverters typically

cause instabilities in inverter-based microgrids. This, so-called, critical clusters, are identified by the eigenvectors of the weighted admittance matrix. Therefore, our method allows us to assess stability and determine the most critical parts of the system in a single step.

We have validated and illustrated our method on a particular system of 4 inverters and demonstrated, that variation only of the very specific parameters can stabilize the system or enhance its stability margin. The developed method has an excellent practical perspective as a method for "weak spots" identification in nearly built microgrids, or microgrids with planned reconfiguration. Further research will focus on deriving closed-form expressions for stability enhancement rules, considering the possible worst-case scenarios in R/X ratios and/or frequency/voltage droop ratios, that can potentially allow formulating robust stability assessment methods.

REFERENCES

- [1] N. Pogaku, M. Prodanović, and T. C. Green, "Modeling, analysis and testing of autonomous operation of an inverter-based microgrid," *IEEE Transactions on Power Electronics*, vol. 22, no. 2, pp. 613–625, 2007.
- [2] E. Barklund, N. Pogaku, M. Prodanovic, C. Hernandez-Aramburoand, and T. C. Green, "Energy management in autonomous microgrid using stability-constrained droop control of inverters," *IEEE Trans. Power Electron.*, vol. 23, no. 5, pp. 2346–2352, 2008.
- [3] V. Mariani, F. Vasca, J. C. Vásquez, and J. M. Guerrero, "Model order reductions for stability analysis of islanded microgrids with droop control," *IEEE Trans. Ind. Electron.*, vol. 62, no. 7, pp. 4344–4354, 2015.
- [4] I. P. Nikolakakos, H. H. Zeineldin, M. S. El-Moursi, and N. D. Hatziargyriou, "Stability Evaluation of Interconnected Multi-Inverter Microgrids Through Critical Clusters," *IEEE Transactions on Power Systems*, vol. 31, no. 4, pp. 3060–3072, 2016.
- [5] M. Rasheduzzaman, J. A. Mueller, and J. W. Kimball, "Reduced-order small-signal model of microgrid systems," *IEEE Trans. Sustain. Energy*, vol. 6, no. 4, pp. 1292–1305, 2015.
- [6] P. Vorobev, P. Huang, M. Al Hosani, J. L. Kirtley, and K. Turitsyn, "High-fidelity model order reduction for microgrids stability assessment," *IEEE Transactions on Power Systems*, vol. 33, no. 1, pp. 874–887, Jan 2018.
- [7] P. Vorobev, P.-h. Huang, M. A. Hosani, J. L. Kirtley, and K. Turitsyn, "A framework for development of universal rules for microgrids stability and control," in *2017 IEEE 56th Annual Conference on Decision and Control (CDC)*, no. Cdc. IEEE, dec 2017, pp. 5125–5130.
- [8] X. Guo, Z. Lu, B. Wang, X. Sun, L. Wang, and J. M. Guerrero, "Dynamic phasors-based modeling and stability analysis of droop-controlled inverters for microgrid applications," *IEEE Trans. Smart Grid*, vol. 5, no. 6, pp. 2980–2987, 2014.
- [9] F. R. Chung and F. C. Graham, *Spectral graph theory*. American Mathematical Soc., 1997, no. 92.
- [10] J. H. Chow, *Power system coherency and model reduction*. Springer, 2013.
- [11] F. R. Gantmakher, *The theory of matrices*. American Mathematical Soc., 1959, vol. 131.